

Supplementary Information

Hybrid organic-inorganic layered TiO₂ based nanocomposite for sunlight photocatalysis

Eglantina Benavente^{a,e}, Carlos Maldonado^{a,e}, Sindy Davis^{b,e}, Leslie Díaz^{c,e}, Harold Lozano^{b,e}, Clivia Sotomayor-Torres^d and Guillermo González^{b,e}.

^a Universidad Tecnológica Metropolitana, P.O. Box 9845, Santiago, Chile.

^b Universidad de Chile, P.O. Box 653, Santiago, Chile

^c Universidad de Santiago de Chile, P.O. Box 10233, Santiago, Chile

^d Catalan Institute of Nanotechnology (CIN2-CSIC) Campus Bellaterra, Spain

^e Center for the Development of Nanocience and Nanotechnology, CEDENNA, Santiago, Chile

Contents.

1. Experimental Section.
2. Characterization
3. Photocatalysis decomposition MB
4. Figures
5. References

1. Experimental section

1.1 Preparation of layered hybrid titanium nanocomposite (LHTiO₂)

In the synthesis, 6.4 g of stearic acid was mixed with 23 mL of ethanol in argon atmosphere, the solution was stirred during 3h at 50 °C. Then were added 4.5 mL of titanium tetraisopropoxide (TTIP) dropwise, and the suspension was stirred for 1 hour at same temperature and repose for one week at 25 °C. The resulting white precipitate was separated by centrifugation, washed three times with ethanol, and dried at 45°C for 72 h. Elemental Analysis for TiO₂(C₁₈H₃₅O₂)_{1.1} x 0.6 H₂O x 0.1(C₁₈H₃₅O₂). Calc.(%): C, 61.80; H, 10.37. Found (%): C, 61.80; H, 10.36; TiO₂: 19.6 (calculated on the basis of thermogravimetric analysis)

1.2. Preparation of CdS nanoparticles (CdS NPs)

The nanoparticles were synthesized by a reported method in the literature, using cadmium chloride and sodium sulfide were taken as cadmium and sulfur sources, respectively.¹

1.3. Preparation of nanocomposites LHTiO₂/CdS NPs

Four suspensions in water:ethanol 1:1 containing each one 0.50 g of TiO₂ (stERIC acid) nanocomposite and proportion 0.1, 0.05, 0.025 and 0.0125 mole of CdS NPs, respectively, were sonicated for 30 seconds. Resulting solids were separated by centrifugation, and thereafter dried at 45 °C for 72 h.

2. Characterization

X-ray diffraction analyses (XRD) of the products were performed using a Siemens diffractometer D-5000 (Cu K α λ = 1.5418 Å). The images of Scanning Electron Microscopy (SEM) and Transmission (TEM), were obtained by using the microscopes EVO MA 10 ZEISS and a JEOL JEM 2200FS (200 kV), respectively. The samples for TEM analysis were prepared by depositing and drying the on a Cu grid a slurry prepared by dispersing the product in ethanol. Raman spectra were obtained by using Raman Alpha300, WITec GmbH in pellets/disks of solid samples using a laser wavelength excitation of 532 nm at room temperature. The diffuse reflectance UV–vis spectra were recorded in the range 200-800 nm at medium scan rate and a slit 0.1 nm at room temperature, using a Shimadzu UV-vis spectrometer, model 2450PC. Barium sulphate was used in all the cases as reference material. Reflectance measurements were converted to absorption spectra using the Kubelka-Munk function.

Kubelka–Munk equation $F(R) = (1-R)^2 / 2R$, where R is the reflectance; $F(R)$ is proportional to the absorption coefficient.² A modified Kubelka–Munk function can be obtained by multiplying the $F(R)$ function by $h\nu$, using the corresponding coefficient (n) associated with an electronic transition as follows: $(F(R)*h\nu)^n$. By plotting the Tauc equation as a function of the energy in eV, the band gap of semiconductor particles can be obtained, E_g was determined as the energy coordinate of the point on the low energy side of curve at which the linear increase starts.³

3. Photocatalytic decomposition of MB

The photocatalytic activity of the products was evaluated by measuring the degradation of methylene blue (MB) aqueous solution under sunlight.

Experiments were performed between at 11.00 am and 16:00 pm (UCT-3), Chilean Summer (Nov–January), under clear sky, with Sun index 8 ([www.woespana.es/Chile/Santiago de Chile](http://www.woespana.es/Chile/Santiago%20de%20Chile)), at 25o C (measured at the site where the experiment was performed). The suspension was irradiated through a borosilicate glass round flask of 100 mL under direct sunlight for a minimum of 3 hours. The constant agitation of the suspension was performed by magnetic stirring, enough for ensuring a high homogeneity of the photocatalyst.

In a typical experiment, 100 mg of the LHTiO₂/CdS NPs were added at 50 mL of 8x10⁻⁶ molL⁻¹ methylene blue aqueous solution in the reaction container. Prior to irradiation, the suspension was magnetically stirred in dark for 30 min to establish an adsorption/desorption equilibrium. Then samples were taken out every 15-20 min and the concentration of MB in supernatant was analyzed by absorption at 665 nm from the UV-visible spectra of the solution (Perkin Elmer Lambda 35), using nanopure water as reference.

The photocatalyst stability of the sample LHTiO₂/CdS NPs was tested. After the first cycle, the catalyst was separated, washed with water-ethanol mixture, dried, and tested again under the same photocatalytic conditions.

The control experiments with scavengers, tert-butyl alcohol (TBA) and benzoquinone (BQ), were performed following the same protocol described above, but in presence 0.1mmol of the scavenger,⁴ and using a simulator solar (Sciencetech SS 150W) instead of sunlight, equipped with an 150W ozone free xenon bulb that produces an AM 1.5 spectrum at an intensity of 1000 W/m² (1sun).

4. Figures

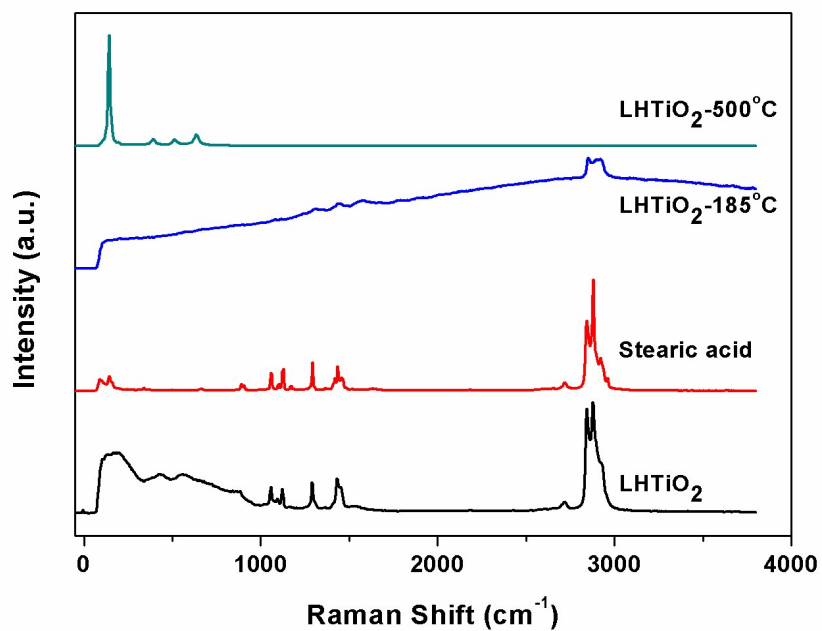


Fig. S1 Raman scattering data of LHTiO₂, stearic acid, LHTiO₂ calcined at 185 °C and 500°C

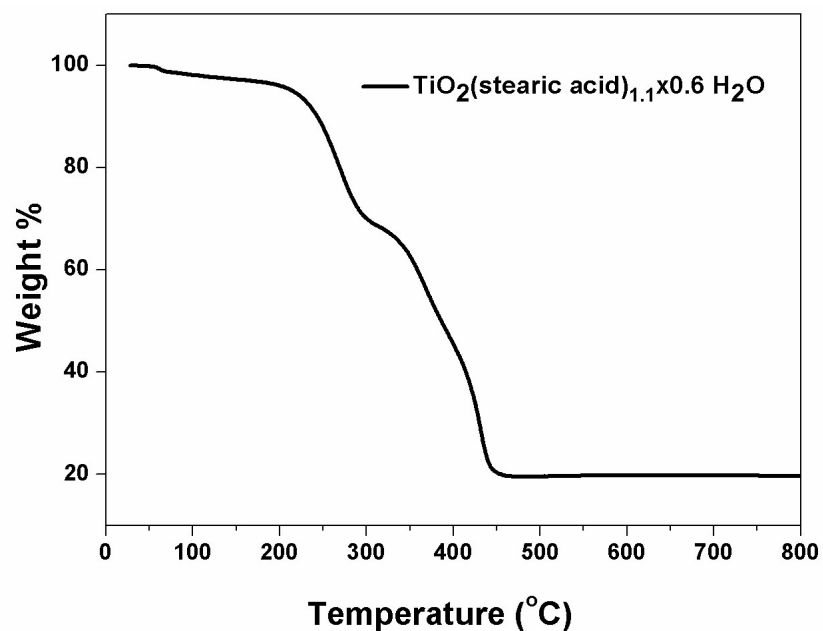


Fig. S2 Thermogravimetric analysis of LHTiO₂

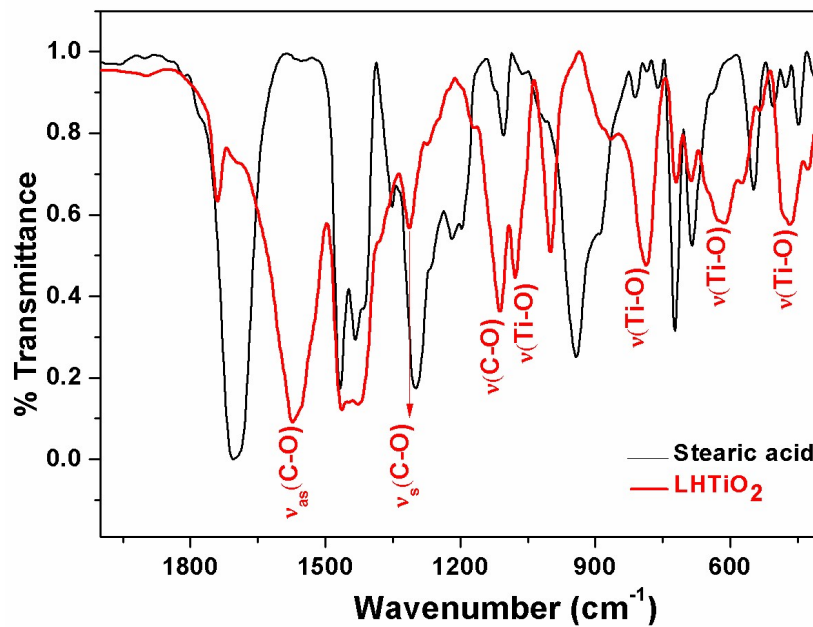


Fig. S3 Infrared spectrum of LHTiO₂ and stearic acid.

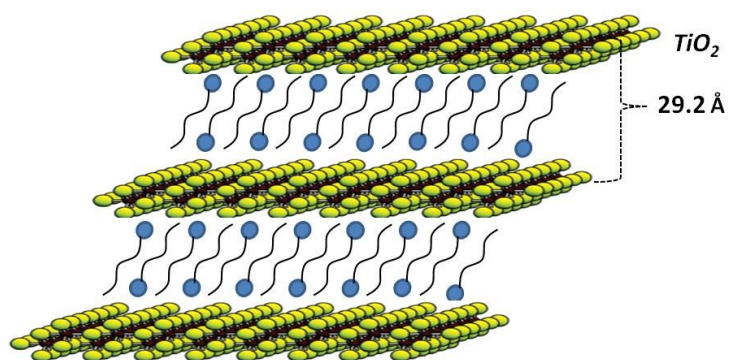


Fig. S4 Schematic representative nanostructure.

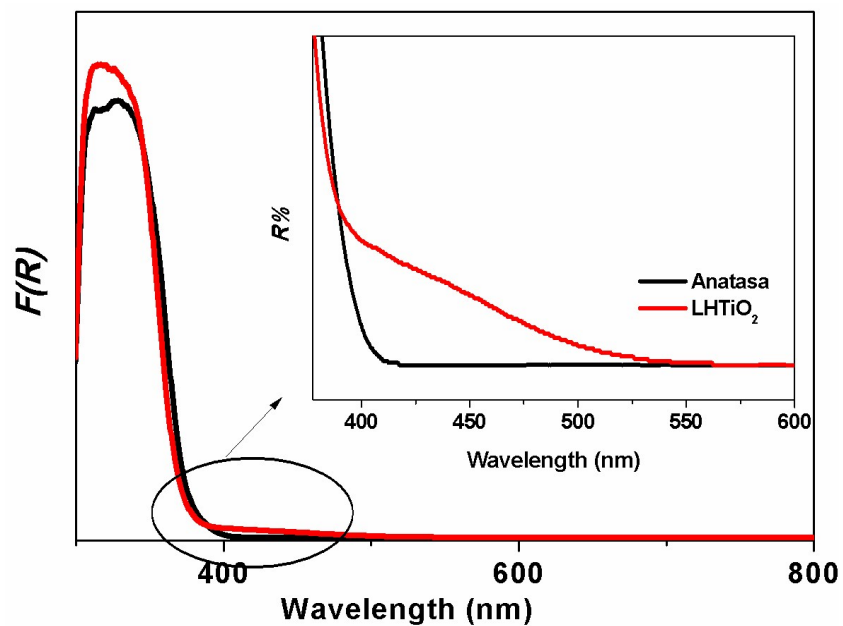


Fig. S5. UV-vis diffuse-reflectance spectra of samples of as-prepared LHTiO₂ and TiO₂ anatase. In insert the extent absorption band.

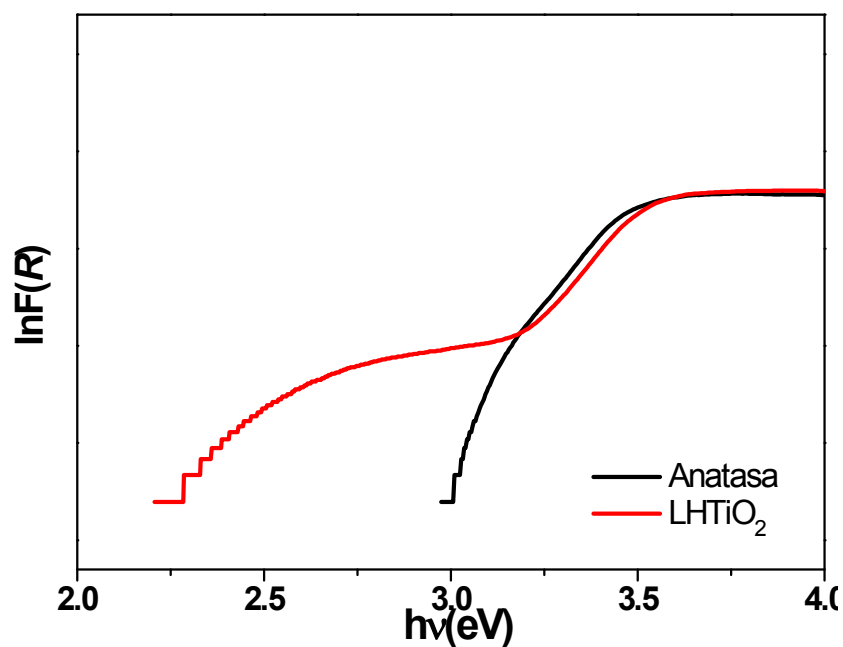


Fig. S6. The relation between absorption coefficient $\ln F(R)$ and energy $h\nu$ for the TiO₂ anatase and LHTiO₂

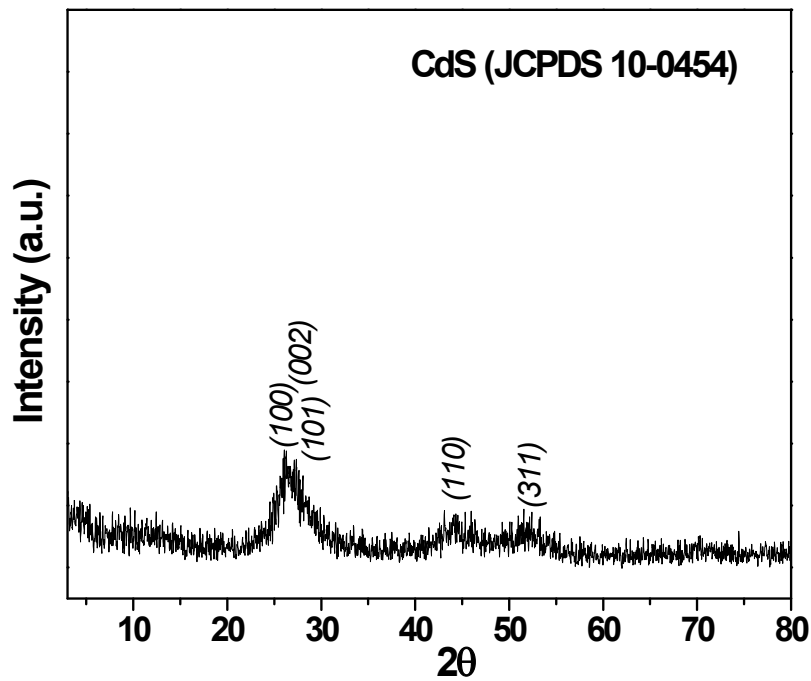


Fig. S7. Power XRD patterns of CdS nanoparticles

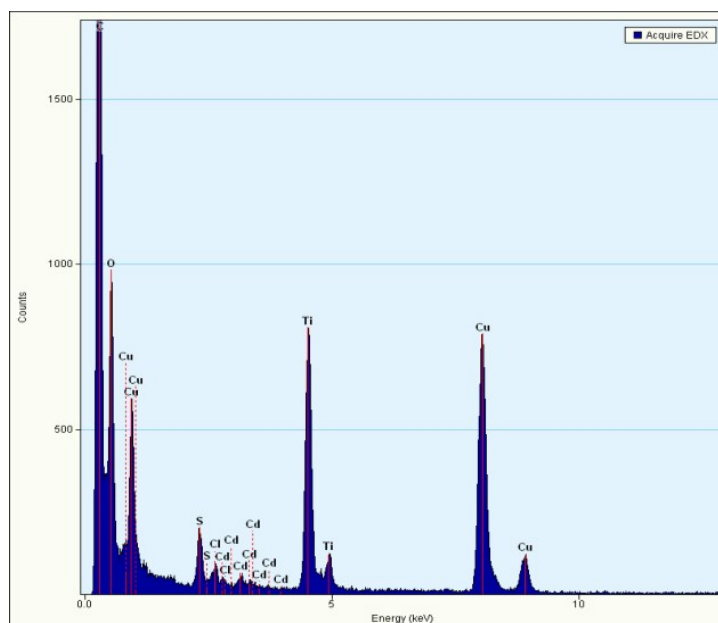


Fig. S8. Energy Dispersive X-ray (EDX) microanalysis of LHTiO₂/CdS NPs

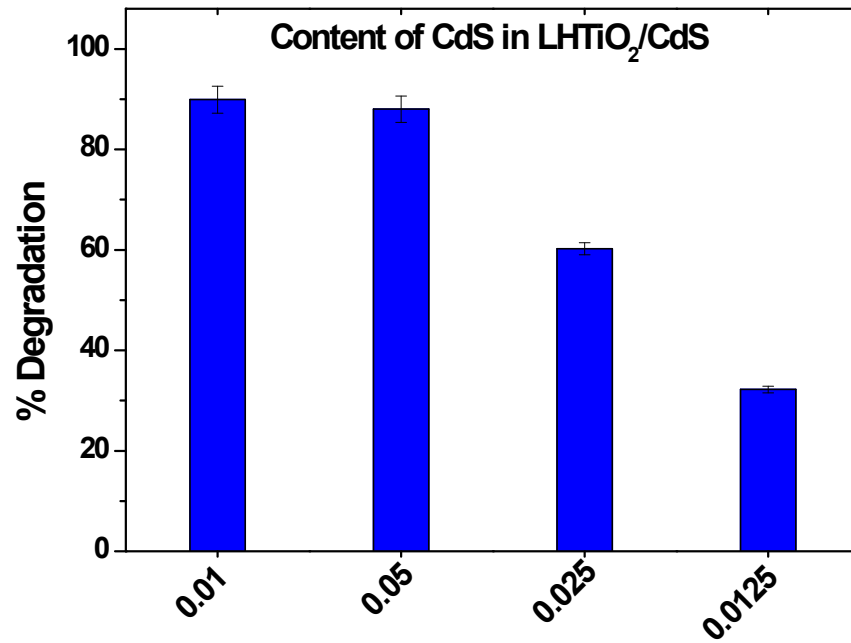


Fig. S9. Degradation of MB with content of CdS NPs (standard deviation of triplicate measurements)

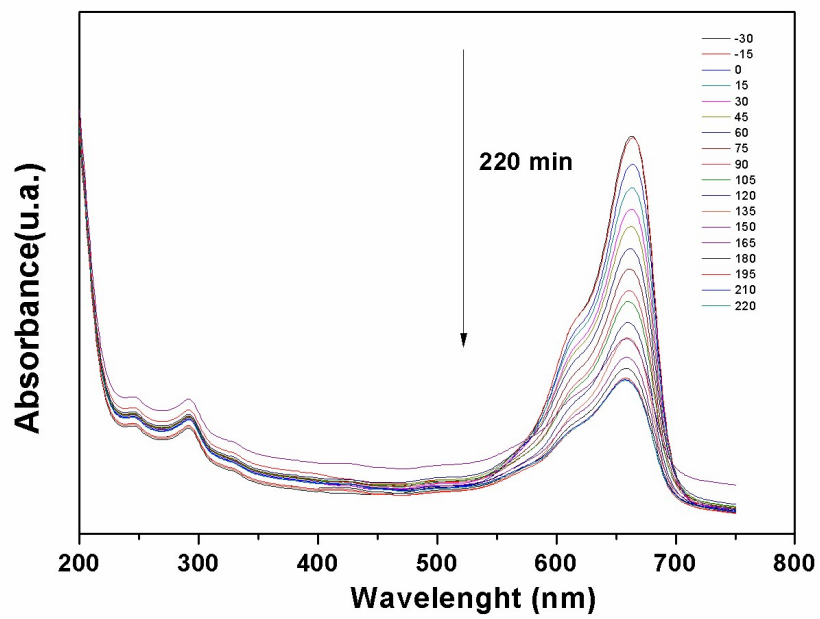


Fig. S10. UV-vis degradation of MB of LHTiO₂/ CdS.

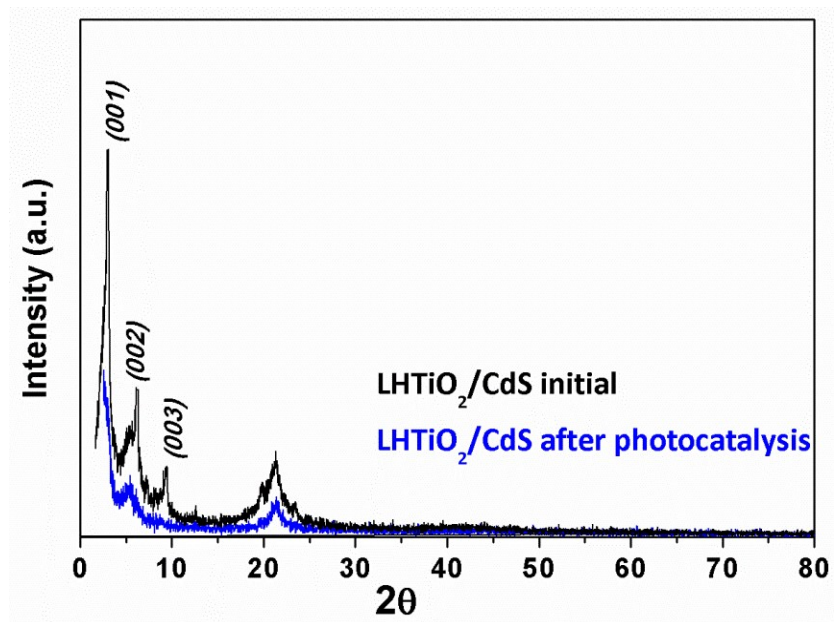


Fig. S11. XRD of LHTiO₂/ CdS after photocatalysis

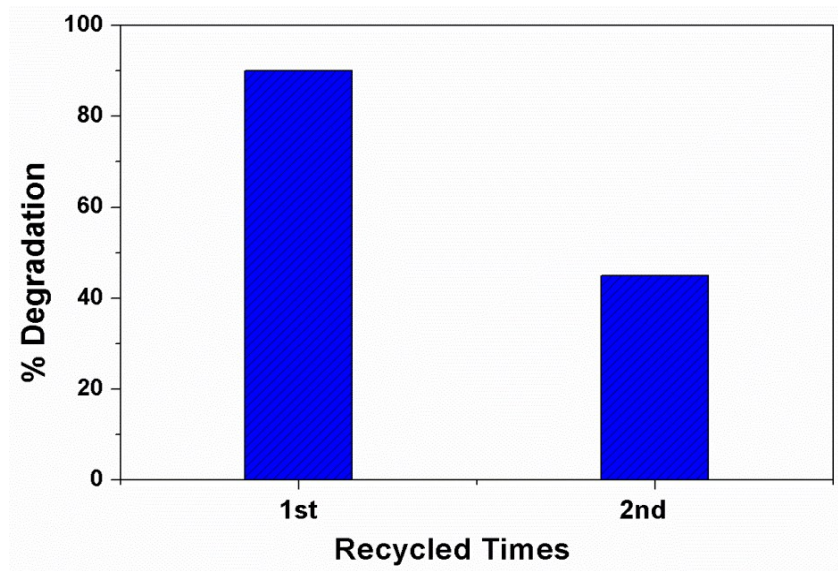


Fig. S12. Recycled test of MB photodegradation under visible irradiation.

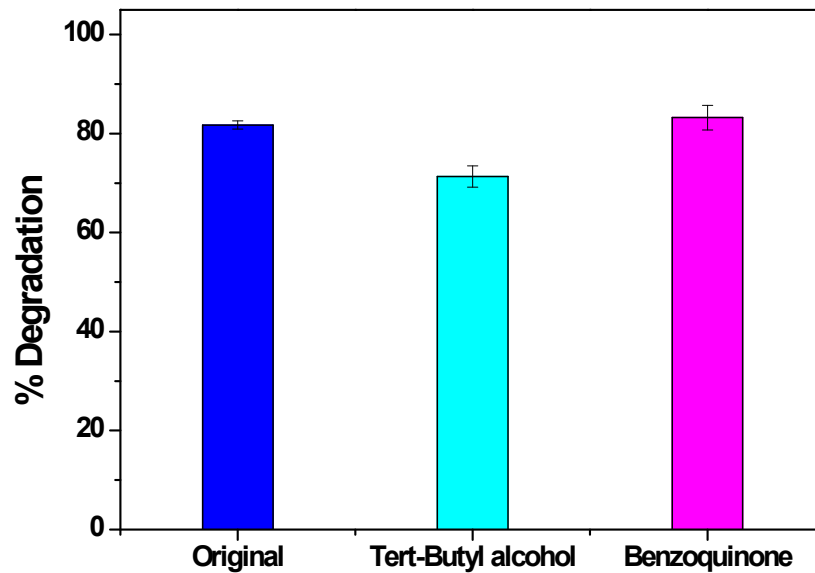


Fig. S13. Photocatalytic degradation of MB in the presence of scavenger ter-butyl alcohol and benzoquinone. Original is the reaction in the absence of any radical scavengers. (standard deviation of triplicate measurements)

5. References

6. P. Chandran, P. Kumari, S. Sudheer Khan, *Solar Energy*, 2014, **105**, 542–547.
7. J.H. Nobbs, *Rev. Prog. Coloration*, 1985, **15**, 66-75.
8. J.Tauc, A. Mentha A. *J Non Cryst. Solids*, 1972, **8-10**, 569-585
9. Zhang, N. Liu, *J.Phys. Chem C*, 2011, **115**, 9136-9145